Luminescence efficiency of *F* centers in KI studied by lifetime measurements

Norio Akiyama and Keita Kobashi
Department of Electrical and Electronic Engineering, Okayama University of Science, Okayama 700-0005, Japan

Shinji Muramatsu
Department of Electrical and Electronic Engineering, Utsunomiya University, Utsunomiya 321-8585, Japan

(Received 26 June 2009; revised manuscript received 23 October 2009; published 25 November 2009)

The luminescence efficiency of isolated *F* centers in KI was studied as a function of the excitation energy by measuring the lifetime for ordinary luminescence. The emission intensity measured under a pulse excitation was found to obey nonexponential decay. The luminescence efficiency decreases to below unity when the excitation energy exceeds 1.96 eV, which corresponds to the slope position at the higher energy side of an *F* absorption band. The threshold value for the luminescence efficiency is lower than that previously obtained from cw measurements but close to that predicted theoretically by Leung and Song. We have traced the origin of this difference by performing experiments based on the cw method and found out the reason. It is shown that there is a relationship between quantities obtained by the cw method and those obtained by our lifetime measurement. Our experimental data are thoroughly analyzed using a model for the radiationless process of Leung and Song, which is based on a 1*s*-2*p* model. A 1*s*-2*p*-2*s* model is also discussed.

DOI: 10.1103/PhysRevB.80.195116 PACS number(s): 61.72.jn, 78.47.Cd, 31.50.Df

I. INTRODUCTION

In general, solid-state laser-type materials are insulators that contain optically active impurity ions or color centers. It is essential to know the luminescence mechanism of activators in matrices. In particular, to search for efficient laser materials, radiationless processes that affect the luminescence efficiency have to be clarified.[1]

Since Dexter *et al.*[2] proposed a criterion for quenching of the emission using a configuration coordinate model, several experimental[3–21] and theoretical[22–28] investigations of the radiationless processes in *F* center[29,30] (point defect that consists of an electron trapped at an anion vacancy) in alkali halide crystals were performed. In order to explain the radiationless process, we sketch an optical cycle in *F* centers using a 1*s*-2*p* (two-level) model, as shown in Fig. 1.[8,9] An electron in an *F* center is optically excited from A [the lowest vibronic state in the ground state (GS)] to B [Franck-Condon state (FCS) in the excited state (ES)]. The excited electron relaxes rapidly from B to C [the lowest level of the relaxed excited state (RES)], accompanying phonon emission, and then goes to D (unrelaxed GS), emitting a photon. Finally, it returns to the initial state A to complete the optical cycle.

The following five typical radiationless processes occur during the optical cycle described above.

(1) *Crossover process.*[2,22] It occurs from a 2*p* to 1*s* potential through a crossing point X_c in Fig. 1, which does not contribute to luminescence. The criterion for judging whether a crystal with *F* centers is luminous or nonluminous was proposed by Bartram and Stoneham[22] and was determined from the relationship between the magnitudes of the optical absorption energy E_{AB} and lattice relaxation energy E_{LR}, as illustrated in Fig. 1. The luminous crystals with *F* centers satisfy the condition $1/4 > \Lambda$, where Λ is a ratio E_{LR}/E_{AB}, while crystals that fail to satisfy that condition are nonluminous.

(2) *Tunneling process.*[23,25] It occurs from the lowest RES to the 1*s* state through the barrier denoted by X_t in Fig. 1 or other neighbor defects, such as *F'* centers (two electron center).[4,5] This process occurs even if the *F* center concentration is low because the wave function of excited states of *F* centers spreads.[31]

(3) *Thermally activated ionization process.*[3,7] Ionization occurs from the lowest RES to the conduction band, which is active at higher temperatures.

(4) *Energy transfer.*[16] Energy of excited *F* centers is transferred to F_2 or *N* centers. This process becomes active in the case of high *F* center concentration.

(5) *Metastable state process.*[14] This is a return to GS before reaching C because of the existence of metastable states, such as F_A centers.[32–34]

In this paper, we focus on isolated *F* centers. Therefore, we pay attention to radiationless processes (1) and (2).

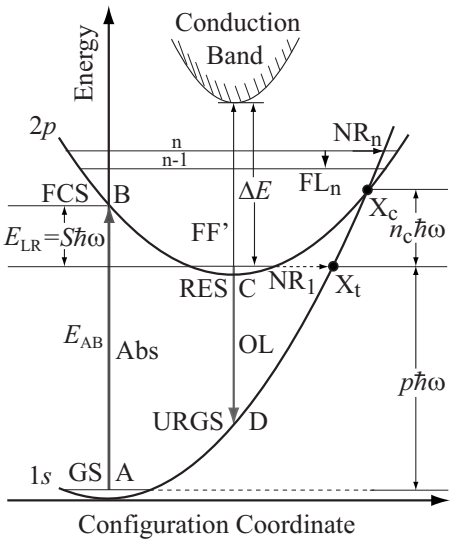

FIG. 1. Schematic diagram of the optical cycle based on a 1*s*-2*p* model.

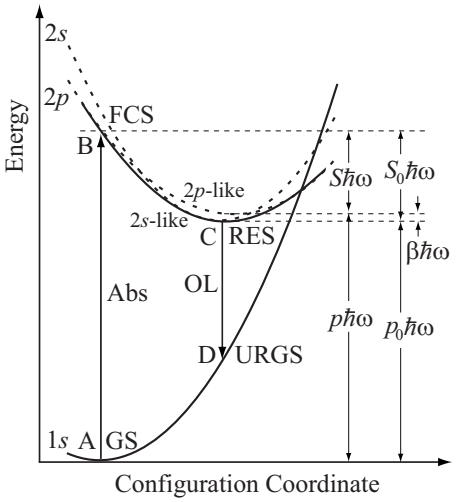

FIG. 2. Schematic diagram of the optical cycle based on a $1s$-$2p$-$2s$ model. $\beta\hbar\omega$ denotes the energy difference between the $2p$-like and $2s$-like states in the RES. $S_0(=S+\beta)$ and $p_0(=p-\beta)$ are introduced.

Most studies on radiationless processes in F centers have been conducted within the framework of the $1s$-$2p$ model.[2,4–14,22–26] However, in a recent development, the role of the $2s$ state in the ES has been recognized and a $1s$-$2p$-$2s$ (three-level) model, as illustrated in Fig. 2, has been proposed.[19] In addition, time-resolved measurement of the radiationless process advanced our understanding of the relaxation mechanism in the ES.[17–21] We understand the deexcitation process of the F center as follows.[19] The phonon wave packet (PWP) associated with the optical excitation of an F electron to the FCS relaxes on the $2p$-potential surface toward the RES with emitting hot luminescence (HL)[19] and transfers from the $2p$ potential to $2s$-like potential at the first crossing point of the $2p$ and $2s$ potentials. After reaching the minimum position of the RES at which ordinary luminescence (OL) occurs, the PWP undergoes a damping oscillation around it.

A recent report, however, suggests that part of the PWP relaxes along the $2p$-potential surface without going to the $2s$-like potential, so that the emission from a $2p$-like state occurs.[20] Koyama *et al.*[20] measured and analyzed time evolution of the HL by femtosecond pulse excitation in the F center in KI. Their result suggests that for the time evolution for the damping oscillation of PWP near 0.15 fs, the luminescence efficiency becomes much smaller than 1 for the excitation energy of 1.823 eV, as shown in Fig. 6(a) in Ref. 20. In other words, their result suggests that the luminescence is quenched at an excitation energy of 1.823 eV.

Next, we focus on the luminescence efficiency for the F center in the KI crystal. According to criterion of Bartram and Stoneham,[22] this F center has $E_{AB}/4=49\hbar\omega$ and $E_{LR}=43\hbar\omega$ ($\hbar\omega$ denotes effective phonon energy, which is 9.5 meV in Ref. 9); both the values are quite close. Therefore, KI crystal provides a borderline case in which OL is suppressed by radiationless processes for excitation energies near the high-energy end of the F band. Wakita and co-workers[8,9] measured the energy dependence of the luminescence efficiency using cw light on the F center in KI. They also performed measurements for the F centers in KBr and NaCl crystals, where luminescence efficiency is expected to exhibit no energy dependence. Wakita and co-workers obtained the luminescence efficiency from the ratio $I_e(E_{ph})/I_a(E_{ph})$, where $I_e(E_{ph})$ and $I_a(E_{ph})$ are the emission and absorption intensities, respectively.[8,9] As mentioned later in Sec. IV, the luminescence efficiency deduced from this method is quite sensitive to the shape of the absorption spectrum, and this may result in a non-negligible error. Two important results they obtained are that the luminescence efficiency of the F center in KI is unity up to the energy of 2.10 eV, which is much greater than the F absorption band peak energy (1.87 eV), and luminous efficiency decreases down to around 0.5 for energy higher than 2.10 eV. Hereafter, we refer to the energy where the luminescence efficiency begins to drop as the dropping energy. Leung and Song[23] theoretically predicted from their two-level model that the dropping energy for the F center in KI is 1.95 eV.

The main objective of this study is to resolve the disagreement of the dropping energy for the luminescence efficiency between previous results reported by Wakita and co-workers,[8,9] Leung and Song,[23] and Koyama *et al.*[20] Therefore, we have performed an experiment by a method different than that used by Wakita and co-workers.[8,9] Our method is based on the measurement of the lifetime of OL and has the merit in that the lifetime is not affected by the F absorption intensity and the luminescence efficiency can be obtained from the ratio of lifetimes alone.[35]

We found that the decay curve of the emission intensity for OL consists of fast and slow components and attributed the fast component to a different center than the isolated F center. We also performed measurements based on the cw method and traced the origin of non-negligible error that may appear when the cw method is used. These results are shown in Sec. IV. In Sec. V, our result of luminescence efficiency is compared with that of Wakita and co-workers and calculation of Leung and Song. Our result of dropping energy is also compared with that of Koyama *et al.* Finally, the $1s$-$2p$-$2s$ model is discussed.

II. EXPERIMENTAL

We used KI crystals with F centers, which were prepared by electrolytic coloration.[36] The sample dimensions were about $3.0\times3.0\times1.5$ mm^3. The F concentration N_F was from 1.5×10^{16} to 1.4×10^{17} cm^{-3}. We quenched the sample from 412 °C to room temperatures to obtain uniform F centers. As shown in Fig. 3, an excitation light pulse from a cavity-dumped dye laser was used (Coherent Antares 7220&702, dye: Rhodamine 6G or DCM special, pulse duration of ~8 ps, tuning range of 560–660 nm), which was excited by the second harmonics of a mode locked Nd^{3+}:YAG laser (Coherent Antares 76s). The repetition frequency of the excitation light pulse was 216 kHz for detecting only one optical cycle of the F center. In order to measure only an F emission band, the emission from a sample of KI crystal, which was installed in a temperature-controlled (Oxford ITC-502, control temperature of 0.1 K) cryostat

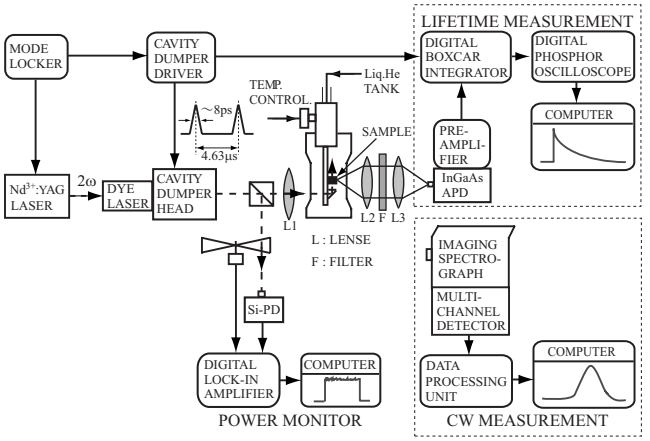

FIG. 3. Block diagram of lifetime and cw measurements.

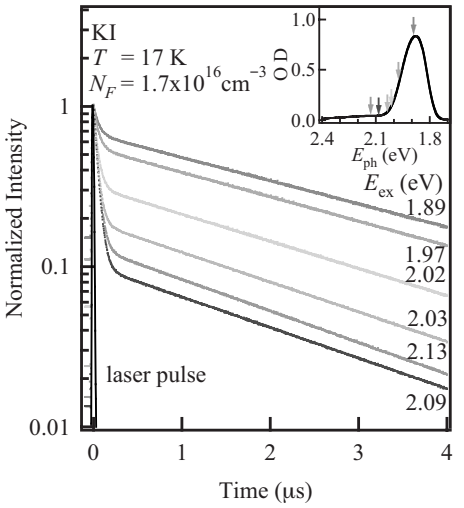

FIG. 4. Time-decay curves of the emission intensity for various excitation energies. The arrows in inset indicate the energy position of excitation in an *F* absorption band. The thin solid line shows a laser pulse shape.

(Oxford Microstat He), was detected with a high-speed infrared detector (Hamamatsu Photonics G8931-20) after it passed through an infrared filter (Schott RG1000). After the detected signal was amplified by a preamplifier (Hamamatsu Photonics C4159-02), it was accumulated by a digital boxcar integrator (NF Electronic Instruments BX-531). In order to improve the signal-to-noise ratio, the output from the digital boxcar integrator was processed through the multiplication of a wave pattern with a digital oscilloscope (Tektronix TDS5104B). Total time resolution of all devices was 19 ns. The temperature of the sample was monitored by a carbon resistor thermometer (Allen-Bradley, 200 Ω, 1/8 W) placed near the sample and a temperature sensor in Oxford ITC-502 (27 Ω rhodium-iron resistance sensor). The carbon resistor was calibrated by using liquid He and liquid N temperatures and the calibrated rhodium-iron resistance sensor in ITC-502. The resistor was measured by a digital multimeter (ADCMT 7461A) or a digital tester. The lowest temperature of our cryostat was 17 K. We carried out measurements mainly at 17 or 25 K, which are higher than those used by Wakita and co-workers,[8,9] but this modification did not interfere with our experimental results.

For the cw measurement as shown in Fig. 3, we set the same repetition frequency of the excitation light pulse as that mentioned above, and the readout time of the video signal for one channel of a multichannel detector with an InGaAs image sensor (Hamamatsu Photonics C5890-256) was set to 400 μs to detect the light passing through a filter (Schott RG1000) and a spectroscope (Jobin Yvon CP200 IR1). The detected signal was accumulated by a personal computer.

The concentration and the absorption bands of the *F* center were measured with an absorption spectrometer (JASCO V-550). Although we performed measurements with the spectral bandwidth from 0.2 to 2 nm, we obtained almost the same results across this range. Then, we used mainly the spectral bandwidth of 1 or 2 nm.

III. EXPERIMENTAL RESULTS OF TIME-DECAY CURVE OF EMISSION

We show a typical experimental result of time-decay curve of the emission for $N_F = 1.7 \times 10^{16}$ cm^{-3} and the excitation energy $E_{ex} = 1.88-2.17$ eV in Fig. 4, where a laser pulse shape is shown by the thin solid line and the *F* absorption band by the solid line in the inset, with arrows indicating the energy position of excitations. For several excitation energies the time-decay curve of the emission is normalized at time $t=0$. We see that the time-decay curve consists of fast and slow components and that the fast component grows as the excitation energy increases. The time-decay curves take a nonexponential form.

The typical temperature dependence of the time-decay curve of the emission for the excitation energy of 1.89 eV, the *F* band peak energy, is shown in Fig. 5. The intensity of the fast component becomes larger and the slope of the slow component becomes steeper as temperature increases.

In Fig. 6, we show the time-decay curve of the emission measured at 25 K for various N_F values from 1.5×10^{16} to

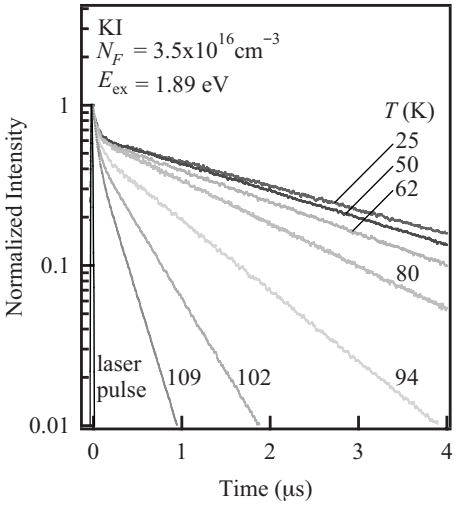

FIG. 5. Typical temperature dependence of the time-decay curve of the emission intensity. The thin solid line shows a laser pulse shape.

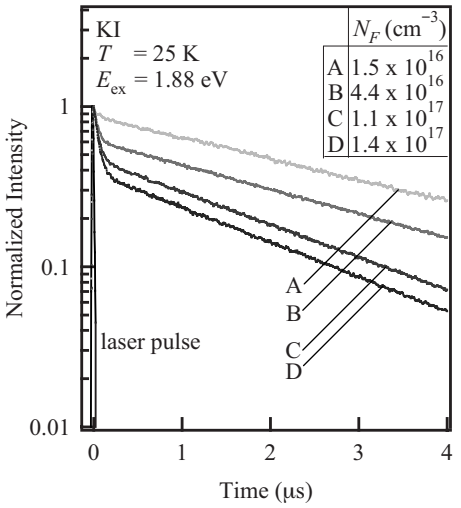

FIG. 6. Concentration dependence of the time-decay curve.

1.4×10^{17} cm^{-3}. Even if N_F is comparatively low (e.g., 1.5×10^{16} cm^{-3}), the time-decay curve appears nonexponential, and the intensity of the fast emission component increases as the concentration increases. Such a tendency of time-decay curves with the variation of the N_F in KI was observed by Fröhlich and Mahr,[37] who obtained the lifetime of ES and the concentration dependence by utilizing a time-recovery phenomenon of absorption light caused by the excitation of the F center in KI.

There exits a difference, however, between their method and ours. Our experimental method is not influenced by a time variation of the number of electrons captured by a metastable state (e.g., F' center) during a radiationless process. According to their result, for a high N_F, the N_F dependence of a time-recovery curve of the absorption intensity becomes nonexponential.[37] However, when the N_F is considerably low (0.8×10^{16} cm^{-3}), the decay obeys a single exponential curve. In our case, when the N_F is 1.5×10^{16} cm^{-3}, we found that the fast component becomes very small. However, the emission decay curve is not a single exponential curve. When the N_F is lower than 1.5×10^{16} cm^{-3}, we cannot observe the emission decay curve because the emission intensity was too small to be observed. Therefore, a single exponential decay curve, which would be obtained in a low-concentrated sample, could not be observed. In Sec. IV, we determine an expression to analyze the nonexponential decay curve.

IV. ANALYSIS OF EXPERIMENTAL RESULTS

A. Dependence of lifetimes on the excitation energy

We extract the lifetime of the emission from the time dependence of the emission intensity $I(t)$ shown in Fig. 4, which is normalized by $I(0)$ for each excitation energy. For this purpose, we have attempted to fit the experimental data to the following four decay types:

(1) decay type resulting from dipole-dipole interactions,
(2) stretched exponential type,
(3) double exponential type, and
(4) double stretched exponential type.

The result of the fitting is summarized in Table I along with function forms used in the fitting. Function form of decay type (1) has been used by Fröhlich and Mahr[37] to explain the nonexponential decay curve obtained from a time-recovery phenomenon of absorption light caused by the excitation of the F center in KI. However, in the present case the residual χ^2 of fitting by use of function form of type (1) is the largest in all the types investigated. On the other hand, the double exponential and double stretched exponential types yield the best fitting. Since the former involves a smaller number of parameters compared to the latter, we selected the double exponential type to obtain the lifetime of the emission. It takes the form

$$I(t) = A_{\mathrm{f}} \exp\left(-\frac{t}{\tau_{\mathrm{f}}}\right) + A_{\mathrm{s}} \exp\left(-\frac{t}{\tau_{\mathrm{s}}}\right). \tag{1}$$

Here, the first and second terms correspond to fast and slow components, respectively. τ_{f} and τ_{s} define lifetimes of the emission, A being a parameter independent of t. We can obtain the values of τ_{f}, τ_{s}, A_{f}, and A_{s} from the fitting of Eq. (1) to the experimental data for each of the excitation energies. The results obtained from such a procedure are shown as a function of the excitation energy, together with the absorption curve of the F band (thin solid line), in Figs. 7(a) and 7(b). We see in the energy region from 1.90 to 2.10 eV that τ_{s} changes significantly, while τ_{f} is almost constant. At 1.96 eV, τ_{s} begins to shorten. In the energy region greater than about 2.15 eV, both τ_{f} and τ_{s} seem to be affected by the presence of the K band. Even if N_F increases, the behavior of the two lifetimes barely changes except that the values of τ_{f} and τ_{s} become slightly smaller. The result of A_{f} and A_{s} will be used in Sec. IV B.

TABLE I. Functions used for fitting the time-decay data of the emission intensity.

Function	Number of parameters	χ^2
$\frac{C_0}{(1+A)\exp(\frac{t}{\tau})-A}$	3	1.72
$A\exp(-\gamma\sqrt{t})$	2	1.05
$A_{\mathrm{f}}\exp(-t/\tau_{\mathrm{f}})+A_{\mathrm{s}}\exp(-t/\tau_{\mathrm{s}})$	4	0.0016
$A_{\mathrm{f}}(\tau_{\mathrm{f}}/t)^{1-n_{\mathrm{f}}}\exp[-(t/\tau_{\mathrm{f}})^{n_{\mathrm{f}}}]$ $+A_{\mathrm{s}}(\tau_{\mathrm{s}}/t)^{1-n_{\mathrm{s}}}\exp[-(t/\tau_{\mathrm{s}})^{n_{\mathrm{s}}}]$	6	0.0014

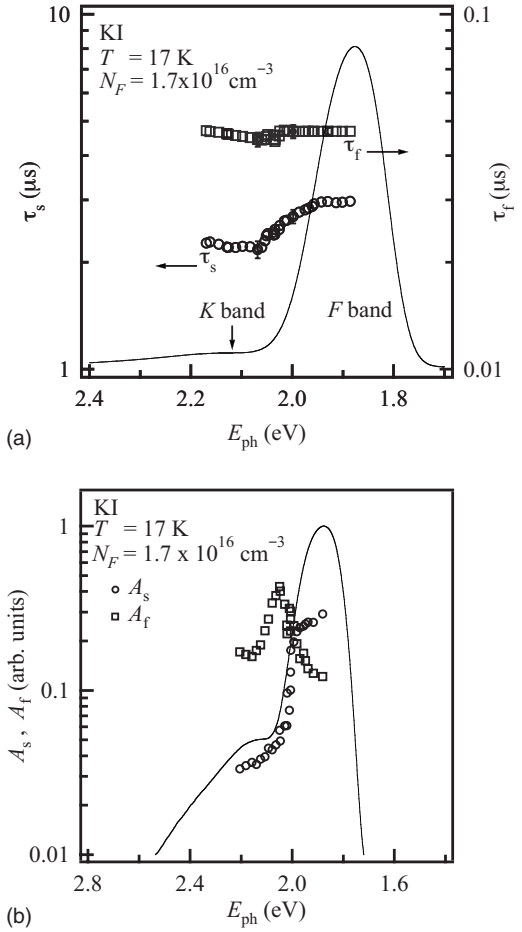

FIG. 7. (a) Dependence of τ_f and τ_s on the excitation energy E_{ph}. (b) Dependence of A_f and A_s on the excitation energy E_{ph}. Solid line shows F band.

B. Excitation spectra calculated from decay intensities

We have obtained excitation spectra for fast and slow components from the results of A_f and A_s shown in Fig. 7(b) by using Eqs. (A4) and (A5) in Appendix, in which the number of irradiation times n is 87 and the duration time t_p is 4.6 μs. They are denoted by $I^{cal}_{cw,f}$ and $I^{cal}_{cw,s}$ respectively, and presented in Fig. 8 as a function of the excitation energy, together with the absorption curve of the F band. We see that $I^{cal}_{cw,s}$ well coincides with the F absorption band except for the high-energy side near the K band. This fact means that $I^{cal}_{cw,s}$ is just the excitation spectrum of slow component and the emission of slow component occurs under thermal equilibrium. The other important fact is that $I^{cal}_{cw,f}$ spectrum with the peak of 2.06 eV is not related to the F absorption band. This result suggests that fast and slow components arise from different sources. The deviation of $I^{cal}_{cw,s}$ from the F band in the high-energy side reflects the decrease in τ_s due to radiationless processes.

In Sec. IV E, we will show that $I^{cal}_{cw,s}$ agrees with the excitation spectrum obtained by the cw method.

C. Dependence of the fast component's lifetime on *F* center concentrations and temperatures

We consider the origin of a fast component that is almost constant in the energy range in which we are interested. The

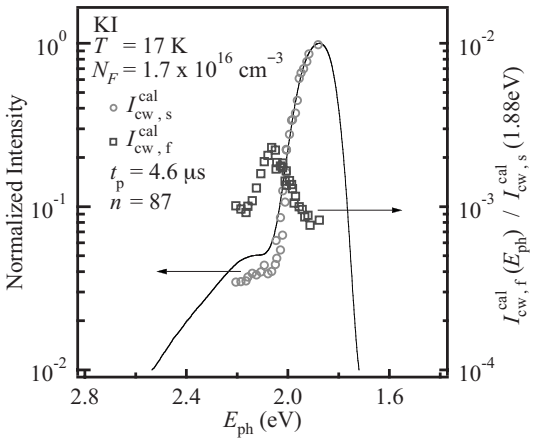

FIG. 8. Excitation spectra for fast and slow components $I^{cal}_{cw,f}$ and $I^{cal}_{cw,s}$. The intensity of $I^{cal}_{cw,f}$ is normalized by the peak intensity of $I^{cal}_{cw,s}$. Solid line shows F band.

previous reports by Bosi *et al.*[38] and a recent one by Koyama *et al.*[20] are important here. Bosi *et al.* measured N_F dependence of the lifetime of F centers in KCl and found that the decay curve was of a single exponential form when N_F was 6.6×10^{16} cm^{-3}, while when N_F was greater than 2×10^{17} cm^{-3}, a fast component appeared because of the generation of F_2 and F_3 centers and tunneling to an F' center. On the other hand, Koyama *et al.*[20] stated that they observed emission from a $2p$-like state of the F center in KI by a femtosecond time-resolved measurement of the HL. Thus, two possibilities exist for the appearance of fast component in the emission lifetime: (1) tunneling to other centers and (2) emission from a $2p$-like state.

In order to determine the origin of the fast component experimentally, we performed lifetime measurements for N_F from 1.5×10^{16} to 1.4×10^{17} cm^{-3}. In Fig. 9, the N_F dependences of lifetimes are shown. It is seen that τ_s decreases, while τ_f remains almost constant, with increasing N_F. The decrease in τ_s can be attributed to the so-called *luminescence quenching*,[5] where an excited electron of an F center tunnels to another F center to form an F' center. On the other hand, the behavior of τ_f seems to suggest that the fast component is related to a different center than the F center because it should decrease, similar to τ_s, if it is related to the F center.

The typical time-decay curves of the emission for different temperatures from 17 to 120 K are shown in Fig. 5, and

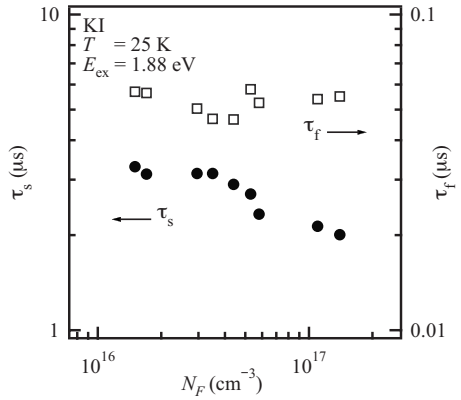

FIG. 9. Dependence of τ_f and τ_s on the concentration N_F.

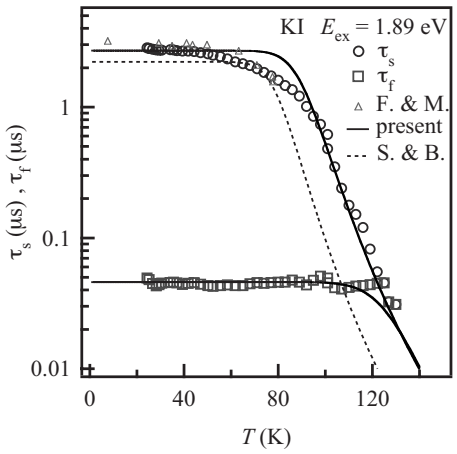

FIG. 10. Temperature dependence of τ_f and τ_s. Data of Fröhlich and Mahr for τ_s is also shown. Fitted lines are calculated by parameters in Table II. Line for the data of Fröhlich and Mahr is not shown, though the parameters are given in Table II.

the lifetimes of the two components are presented as a function of temperature in Fig. 10, where the experimental data of Fröhlich and Mahr[39] are also shown. We note that τ_s abruptly drop near 80 K, while τ_f is independent of temperature in the range of our measurement. τ_s in Fig. 10 is considered to represent the radiative lifetime of OL since in this excitation energy (E_{ph}=1.89 eV) the effect of radiationless processes on τ_s is negligible.

Here, we attempt to fit the radiative-lifetime data in Fig. 10 to the following equation, which is based on thermal excitation of F electrons to the bottom of the conduction band lying above the 2s-like level:

$$\tau = \frac{\tau_R}{1 + \left(\frac{\tau_R}{\tau_0}\right)\exp\left(-\frac{\Delta E}{k_B T}\right)}, \tag{2}$$

where τ_R is the radiative lifetime, $(1/\tau_0)\exp[-\Delta E/(k_B T)]$ is the probability of thermal ionization into the conduction band with activation energy ΔE, and k_B is the Boltzmann factor. The fitting parameters are summarized in Table II, and the fitted line is the solid line in Fig. 10. The small dots indicate the temperature dependence of radiative lifetime, which was measured by Swank and Brown[40] using a photocurrent method. It is seen that the temperature where τ_s starts to drop is different between our study and that of Swank and Brown. We consider that this difference is not due to the difference in N_F but is because of the reflection of an effect of F' centers created by laser irradiation. In fact, Park[41] and Chiarotti and Grassano[42] reported that F' centers were created even at low temperatures by laser irradiation of F centers in KCl. Moreover, Benci and Manfredi[43] studied the temperature dependence of the lifetime for F centers in KCl when there existed the influence of the F' center and reported that the radiative lifetime was larger than that of the isolated F center.

TABLE II. Parameter values obtained from fitting of the temperature dependence of lifetimes.

	ΔE (eV)	τ_R (μs)	τ_0^{-1} (s^{-1})	Ref.
τ_s	0.126	2.70	3.5×10^{12}	Present
τ_f	0.172	0.046	1.2×10^{14}	Present
τ	0.110	3.00	3.5×10^{12}	39
τ	0.110	2.22	3.5×10^{12}	40

On the other hand, a similar phenomenon such that τ_f does not depend on temperatures and has been observed in the temperature dependence of the fast decay component of F centers in KCl and NaBr by Bosi *et al.*[38,44] They reported that the fast component of the emission arose from $M(F_2)$ centers.

Koyama *et al.*[20] reported the fast emission from a 2p-like state of the F center in KI by a femtosecond time-resolved measurement of the HL. However, our result of activation energy ΔE for the fast component is 172 meV, which is greater than that of the slow value of 126 meV. This discrepancy suggests that the 2p-like state is lower than the 2s-like state. Therefore, we can rule out the possibility that the fast emission arises from the 2p-like state.

Our experimental results mentioned above imply that the fast component of the lifetime has a completely different N_F and temperature dependences from those of the slow component. This fact indicates that the slow and fast components cannot be explained within the same framework. We are led to the conclusion that the fast component of emission is not related to isolated F centers, but originates from other centers such as the F_2 or F_3 centers that really emit the light with an energy overlapping that of the F center emission, as was reported in the radiative-lifetime measurement of color centers in KCl and NaBr,[38,44] or indicates the influence on the emission caused by tunneling. We will report details in the near future.

From the above discussion we can say that the fast component of emission is not related to the F band absorption. Similarity of its excitation spectrum $I_{cw,f}^{cal}$ to the K band seems to suggest a possibility that the fast component may be associated with the K band. However, luminescence efficiency of the fast component evaluated by the same method as that used in Sec. IV D near the K band peak prevents us from attributing the fast component to the K band. Therefore, at present we believe that it is related to an unknown center other than the F center, as mentioned in the last paragraph of Sec. IV B.

D. Luminescence efficiency for the slow component

In the preceding subsections we have shown that the lifetime of the slow component τ_s represents the lifetime of the emission from OL of the F center. It is noted that our value of τ_s of about 1.90 eV (2.0 μs) is close to that (1.8 μs at 77 K) obtained by Fröhlich and Mahr[39] as the lifetime of isolated F centers.

Here, we compare our result of τ_s shown in Fig. 7(a) to the previous result[9] of luminescence efficiency η, which is given by the ratio of the lifetime τ to the radiative lifetime τ_R, τ being composed of radiative and nonradiative

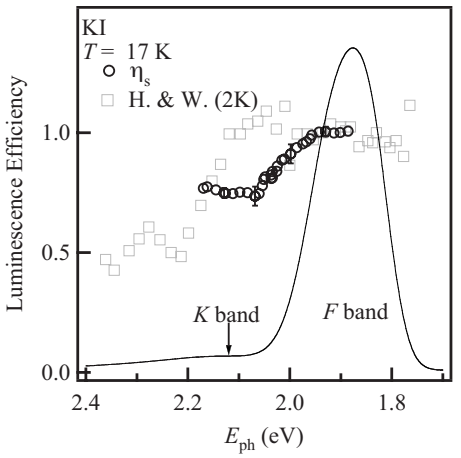

FIG. 11. Spectrum of the luminescence efficiency along with that of Hirai and Wakita.

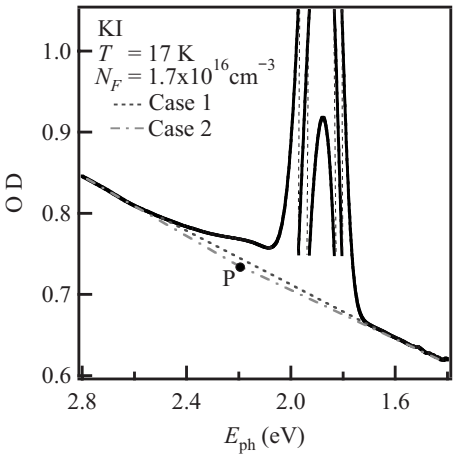

FIG. 12. Fundamental absorption spectrum of the *F* center in KI before background subtraction. Two baselines are shown for the background. The baseline containing point P is referred as case 2, while the other case 1. For details, see the text.

components,[45] by defining relative luminescence efficiency $\eta_s(E_{ph})$ as

$$\eta_s(E_{ph}) = \frac{\tau_s(E_{ph})}{\tau_s(1.90\ \text{eV})}. \tag{3}$$

This becomes 1 when $E_{ph}=1.90$ eV, where τ_s nearly equals τ_R since the contribution of the nonradiative component almost vanishes at $E_{ph}=1.90$ eV. The experimental data are shown as a function of E_{ph} in Fig. 11, where the result obtained by Hirai and Wakita[9] with cw light excitation is also shown by squares. Our result and result of Hirai and Wakita[9] with respect to the E_{ph} dependence are similar, except the dropping energy of luminescence efficiency, which is 1.96 eV in the former and 2.10 eV in the latter, and except the magnitude in the higher excitation energy, which is 0.75 in the former and 0.5 in the latter.

The decrease in luminescence efficiency is due to the increase of a radiationless probability. Figure 11 shows that this increase starts at about 1.95 eV. This change with the variation of excitation energy is quantitatively explained in Sec. V.

E. Luminescence efficiency obtained from the cw method

We found the origin of the disagreement between our experimental result and experimental result of Wakita *et al.* by performing cw measurements. As shown in Appendix, because the excitation spectrum of the isolated *F* center can be obtained, the luminescence efficiency in the cw method at a certain excitation energy E_{ph} is obtained from the ratio of $I_e(E_{ph})/I_a(E_{ph})$, where $I_e(E_{ph})$ and $I_a(E_{ph})$ are emission and absorption intensities, respectively.[8,9] Then, relative luminescence efficiency $\eta_{cw}(E_{ph})$ for the cw method is given by

$$\eta_{cw}(E_{ph}) = \frac{[I_{cw}(E_{ph})]_{norm}}{[I_a(E_{ph})]_{norm}}, \tag{4}$$

where $[I_{cw}(E_{ph})]_{norm}$ and $[I_a(E_{ph})]_{norm}$ are the normalized emission intensity (excitation spectrum) and absorption intensity (absorption spectrum), respectively, obtained from the following:

$$[I_{cw}(E_{ph})]_{norm} = \frac{I_e(E_{ph})}{I_e(1.90\ \text{eV})}, \tag{5}$$

$$[I_a(E_{ph})]_{norm} = \frac{I_a(E_{ph})}{I_a(1.90\ \text{eV})}. \tag{6}$$

The fundamental absorption spectrum of the *F* center in KI has a shape shown in Fig. 12, in the case that the background (absorption of the KI host crystal), denoted by a baseline, is not subtracted. In general, to obtain an absorption curve for the *F* center from the fundamental absorption spectrum, a baseline is drawn to subtract the background. In Fig. 12, two baselines are drawn: first is a single straight line connecting both absorption edges (*case 1*) and the other consists of two straight lines crossing at point P (*case 2*). If the slope angles at the low- and high-energy sides equal each other, these baselines completely coincide. However, this is not the case in *F* centers in KI. In Fig. 13, *F* absorption bands $[I_a(E_{ph})]_{norm}$ (indicated as the dotted lines for case 1 and dashed-dotted lines for case 2, respectively) obtained by subtracting the background with two types of baselines are shown by semilogarithmic plots. We see a noticeable difference in the higher energy region between results obtained after the background subtraction based on the two different procedures. We note that the excitation spectrum $[I_{cw}(E_{ph})]_{norm}$ obtained by the cw method is also shown by a + mark in Fig. 13.

In Fig. 14, luminescence-efficiency spectra obtained by two procedures for the background subtraction are compared with the result of Hirai and Wakita[9] and our result obtained from the lifetime measurement. We have found that the luminescence-efficiency spectrum (indicated as reverse triangles) obtained in case 2 agrees with our result of the lifetime measurement (indicated as black circles), while that obtained in case 1 (marked by triangles) differs from our result, being instead similar to result of Hirai and Wakita.

Furthermore, there is a relationship between quantities obtained from the cw method and our lifetime measurement.

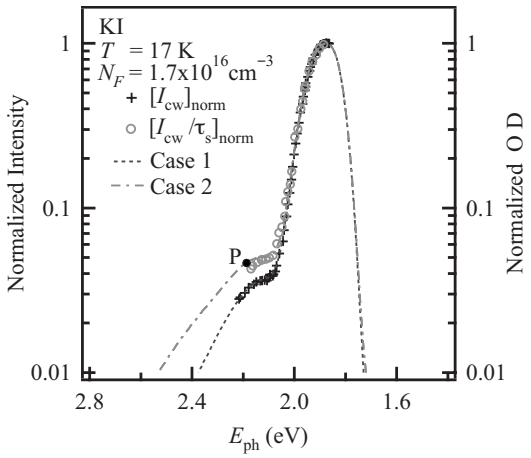

FIG. 13. F absorption bands $[I_a(E_{ph})]_{norm}$ obtained by the two different subtraction procedures. For comparison, excitation spectra $[I_{cw}(E_{ph})]_{norm}$ and $[I_{cw}(E_{ph})/\tau_s(E_{ph})]_{norm}$ are also shown by + marks and open circles, respectively.

The ratio of $\eta_{cw}(E_{ph})$ and $\eta_s(E_{ph})$ is, expressed from Eqs. (3)–(6), as follows:

$$\frac{\eta_{cw}(E_{ph})}{\eta_s(E_{ph})} = \frac{[I_{cw}(E_{ph})]_{norm}}{\tau_s(E_{ph})I_a(E_{ph})}\tau_s(1.90\ \text{eV})I_a(1.90\ \text{eV}) \propto \frac{[I_{cw}(E_{ph})/\tau_s(E_{ph})]_{norm}}{I_a(E_{ph})}. \quad (7)$$

Thus, Eq. (7) means that $[I_{cw}(E_{ph})/\tau_s(E_{ph})]_{norm}$ is proportional to the F absorption band when the cw method and the lifetime measurement yield the same result. In Fig. 13, $[I_{cw}(E_{ph})/\tau_s(E_{ph})]_{norm}$ obtained in case 2 is indicated as the circles. It is in good agreement with the F absorption band shown by the dashed-dotted lines.

From the above, we have found that the difference between our experimental result and result of Wakita and co-workers[8,9] arises from a slight difference in the shape of the absorption spectrum caused by a background subtraction procedure.

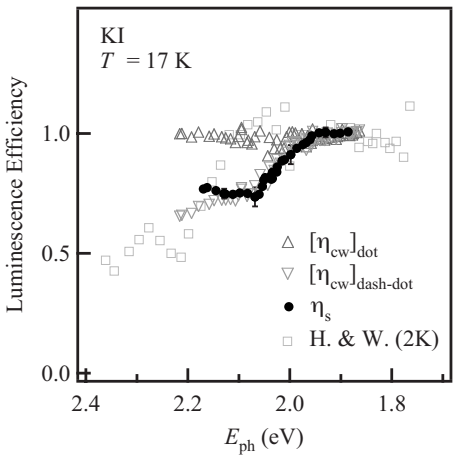

FIG. 14. Comparison between spectra of the luminescence efficiency obtained from the cw method and lifetime measurement.

We notice that the excitation spectrum (in Fig. 13) obtained by the cw method is in good agreement with the $I^{cal}_{cw,s}$ reproduced from lifetime measurements (in Fig. 8). This implies that in the cw measurement only the part corresponding to $I^{cal}_{cw,s}$ is detected since the magnitude of $I^{cal}_{cw,f}$ is quite small compared to that of $I^{cal}_{cw,s}$.

V. COMPARISON OF THE LUMINESCENCE EFFICIENCY BETWEEN EXPERIMENT AND THEORY

In this section, we compare our experimental result for the luminescence efficiency with the model originally proposed by Leung and Song.[23] This model was modified by Hirai and Wakita[9] to incorporate the effect of tunneling to F' center, and they applied it to their experimental result. This model is based on the configuration coordinate that acts as an accepting mode for the vibrational relaxation. It assumes two relaxation routes: first is a step-by-step vibrational transition accompanied by phonon emissions within the $2p$ states and the second a transfer from the $2p$ state to the ground $1s$ state with no emission of light. A back transfer from the $1s$ to the $2p$ state is assumed to be negligibly small.

The expression for the luminescence efficiency η_s of model of Leung and Song, as modified by Hirai and Wakita,[9] is expressed as follows:

$$\eta_s = \prod_{n=n_0}^{1} \eta(FL_n), \quad (8)$$

where

$$\eta(FL_n) = \frac{FL_n}{NR_n + FL_n}, \quad (n = 2, \ldots, n_0), \quad (9)$$

$$\eta(FL_1) = \left(\frac{1/\tau_R}{NR_1 + 1/\tau_R + FF'}\right)(1 - FF'T). \quad (10)$$

Here, NR_n in Eqs. (9) and (10) denotes the probability of the radiationless decay due to the transfer from the $2p$ state to the $1s$ GS and is given by

$$NR_n = W_0 e^{-S} S^p \frac{n!}{(n+p)!}[L_n^p(S)]^2 \quad (n = 1, \ldots, n_0), \quad (11)$$

where W_0 is an appropriate constant determined by the transition matrix element of the promoting mode between the $2p$ and $1s$ states, and the remaining arises from the square of the overlap integral of the two displaced harmonic oscillator wave functions for the n and $(n+p)$ levels associated with $2p$ and $1s$ states, respectively (see Fig. 1). S is the Huang-Rhys factor,[46] which is a measure of the relative displacement between the harmonic oscillators associated with the $2p$ and $1s$ states and is related to the Stokes shift $E_{SS}(=2E_{LR})$ as $S = E_{SS}/(2\hbar\omega)$, where ω is an effective angular frequency of the accepting mode. p is an integer defined by $p = E_{AB}/(\hbar\omega) - S$ (E_{AB} denotes absorption energy; see Fig. 1); in other words, $p\hbar\omega$ denotes the difference between energy

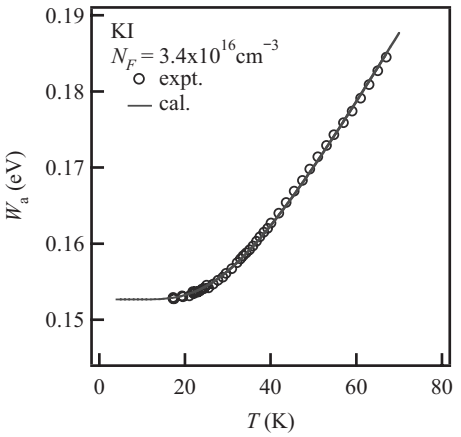

FIG. 15. Temperature dependence of the full width at half maximum for *F* absorption band. The solid line indicates a curve fitted to Eq. (14).

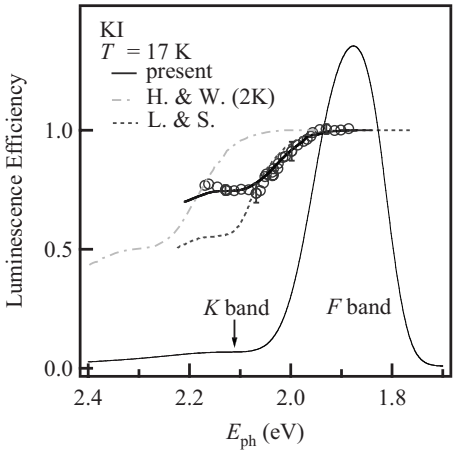

FIG. 16. Comparison of the luminescence efficiency between experiment and calculation with the other results. Solid circles are experimental data.

origins of the vibronic levels for the $2p$ and $1s$ states (see Fig. 1). $L_n^p(S)$ is the Laguerre polynomial.

FL_n in Eq. (9) denotes the step-by-step vibrational transition within the $2p$ state and is

$$FL_n = n\pi\Delta W, \tag{12}$$

where ΔW is a constant value of 10^{10}–10^{12} s^{-1}.[47] $1/\tau_R$ in Eq. (10) is a radiative transition probability from the lowest state. $FF'T$ in Eq. (10) is a probability for the electron tunneling from the lowest RES of the *F* center to the nearest-neighbor *F* center to form the F' center and FF' is a relative probability of the thermal ionization of the *F* center with activation energy ΔE to form F' centers, being given as

$$FF' = \frac{1}{\tau_0}\exp\left(-\frac{\Delta E}{k_B T}\right). \tag{13}$$

The term n_0 in Eq. (8) indicates the level to which an *F* electron is excited, being related to the excitation energy by $E_{ph}=(n_0+p)\hbar\omega$.

Before proceeding to fit Eq. (8) to experimental data, we need to decide which parameters we choose as unknown. In order to reduce unknown parameters, we measured the temperature dependence of the absorption bandwidth W_a, which gave us the values of important parameters $\hbar\omega$ and S. In Fig. 15 the experimental data are plotted along with the fitted curve[48] which is given by

$$W_a(T) = W_a(0)\left[\coth\left(\frac{\hbar\omega}{2k_B T}\right)\right]^{1/2}, \tag{14}$$

where

$$W_a(0) = \hbar\omega[8\ \ln 2 \cdot S]^{1/2}. \tag{15}$$

The values of $\hbar\omega$ and S were determined to be 9.6 meV and 46, respectively, from the best fitted curve.

Now we can compare Eq. (8) with the experimental data. We set $\hbar\omega$=9.6 meV, E_{AB}=1.891 eV,[49] $\pi\Delta W=3.9\times10^{10}$ s^{-1}, and $1/\tau_0=3.5\times10^{12}$ s^{-1} (Table II in Ref. 9). When we use $1/\tau_R=3.7\times10^5$ s^{-1} and ΔE=126 meV from our results in Table II, free parameters reduce to two, that is S and W_0. Then we easily try to fit Eq. (8) to our data. The best fitting was achieved when S=47 and $W_0=0.38\times10^{13}$ s^{-1}, as shown in Fig. 16. Previous results from Hirai and Wakita[9] and Leung and Song[23] are also shown. The parameter values are listed in Table III for comparison with previous results. We note that the value of p is determined from the relation $p=E_{AB}/(\hbar\omega)-S$. Our parameter set reproduces well the experimental result for the luminescence efficiency. The value of S (=47) obtained from the fitting agrees well with that (S=46) from the temperature dependence of the *F* absorption bandwidth. As shown in Table III, the parameter sets used by us and Hirai and Wakita[9] do not differ largely from each other; however, a difference is seen in their resulting curves of η, whose dropping energies are shifted

TABLE III. Values of input parameters used for fitting luminescence-efficiency data to Eq. (8). Values of output parameters are also listed. For details, see the text.

$\hbar\omega$ (meV)	$\frac{E_{LR}}{\hbar\omega}$ S	$\frac{E_{AC}}{\hbar\omega}$ p	$\frac{(p-S)^2}{4S}$ n_c	W_0 (s^{-1})	$\pi\Delta W$ (s^{-1})	τ_R^{-1} (s^{-1})	τ_0^{-1} (s^{-1})	ΔE (meV)	T (K)	$\frac{S}{(p+S)}$ Λ	Ref.
9.6	47	150	56.4	0.38×10^{13}	3.9×10^{10}	3.7×10^5	3.5×10^{12}	126	17	0.239	Present
9.5	43	155	74	1×10^{13}	3.9×10^{10}	4.5×10^5	3.5×10^{12}	110	2	0.217	9
8	54	180	74	1×10^{13}	10^{10}–10^{12}				0	0.231	23

TABLE IV. Relationship of output parameters in Table III and absorption and emission energies. The value of β is determined so that $(p_0-S)\hbar\omega$ agrees with the experimental data of E_{CD}.

				E_{AB}		E_{CD}		
$\hbar\omega$ (meV)	S_0	p_0	β	$(p+S)\hbar\omega$ (eV)	$(p_0+S_0)\hbar\omega$ (eV)	$(p-S)\hbar\omega$ (eV)	$(p_0-S)\hbar\omega$ (eV)	Ref.
9.6	64	133	17	1.891	1.891	0.989	0.826	Present
9.5				1.881		1.064		9
8				1.87		1.008		23
				1.875	1.875	0.827	0.827	49

from each other by about 0.14 eV ($\cong 14\hbar\omega$). This shift probably due to the difference in Λ defined by $S/(p+S)$ (see Table III) because our value and value of Leung and Song of Λ are close to each other, but that of Hirai and Wakita is rather different from them. This fact means that Λ is an important factor for determining the dropping energy of the luminescence-efficiency spectrum.

In the above fitting we used the experimental value of E_{AB} (=1.891 eV) and determined the value of S in addition to those of the parameters that take part in the radiationless process. We are interested in examining whether the determined parameters satisfy the emission energy E_{CD} =0.827 eV.[49] Since E_{CD} is expressed in terms of S, p, and $\hbar\omega$ as $E_{CD}=(p-S)\hbar\omega$, E_{CD} amounts to 0.989 eV. This value is 0.16 eV larger than the experimental value of 0.827 eV.[49] In Table IV, the value of E_{CD} is listed along with that of E_{AB} for comparison with those values deduced from parameter values of Hirai and Wakita.[9]

In order to explain consistently the whole of the optical cycle described in Sec. I, it seems that we have to account properly for the role played by the 2*s* state in the relaxation process. In Fig. 2 the role of the 2*s* state is shown schematically. If instead of $E_{CD}=(p-S)\hbar\omega$, we could consider it as $E_{CD}=(p_0-S)\hbar\omega$ taking account of the energy difference between the 2*p*-like and 2*s*-like states in the RES, which is denoted by $\beta\hbar\omega$ in Fig. 2, the emission energy would decrease. For a more convincing demonstration of the 2*s* state's role, it is highly desirable to extend a 1*s*-2*p*-2*s* model so as to treat both the radiative and nonradiative processes at the same time.

Finally, we make a comment on the experimental result of Koyama *et al.*,[20] who have carried out the time-resolution measurement of HL with femtosecond pulse excitation in the *F* centers (concentration of 5×10^{16} cm^{-3}) in KI. From the time evolution of damping oscillation of the PWP for the excitation energy of 1.823 eV [Fig. 6(a) in Ref. 20], we can read the time that the emission energy becomes zero, that is, 0.15 fs. This means that the PWP arrives at the crossing point of ES and GS at that time. Since the PWP transfers from the ES to the GS at the crossing point, the number of electrons coming back to the bottom of ES and emitting light decreases, so that the emission intensity would begin to decrease. In other words, when the *F* center is excited with the energy of 1.823 eV, it is expected that the luminescence efficiency becomes smaller than unity. However, this does not match our experimental result nor that of Wakita and co-workers.[8,9] We would like to point out the possibility that Koyama *et al.* observed a phenomenon related to the fast emission component as shown in Fig. 4 since their experiment was performed for the *F* centers of considerably high concentration.

VI. CONCLUSION

We have performed lifetime measurements of OL in the *F* center in KI crystal for various excitation energies to investigate the luminescence efficiency. It has been found that the lifetime has two components, fast and slow. We have suggested that the fast component should be attributed to centers other than isolated *F* centers. The spectrum of the luminescence efficiency deduced from the dependence of the slow component on the excitation energy is compared with previous results obtained by the cw method. The present and previous results for the luminescence efficiency disagree particularly in the dropping energy in the luminescence-efficiency spectrum. We have determined the origin of this difference by performing measurements by the cw method. It was found that the absorption spectrum is quite sensitive to background subtraction, so that the resulting luminescence efficiency in the cw method tends to include a non-negligible error. Our experimental data of the luminescence efficiency have been shown to be adequately described by the model of Leung and Song.

In this paper, we have not reported detailed data for the concentration dependence of lifetimes. The study on the concentration dependence remains for future work. At present, we are analyzing the experimental data of the luminescence efficiency using a model that incorporates damping motion of the PWP in a semiclassical 1*s*-2*p*-2*s* model.

ACKNOWLEDGMENTS

The authors wish to thank T. Iida of Osaka City University for valuable discussions. They are also indebted to P. Raerinne for his technical contribution in properly coloring the samples used in the experiments.

APPENDIX

Here we notice that $I_e(E_{ph})$ obtained from our cw measurement using a multichannel detector can be reproduced using lifetime measurement data. When the *F* center is irra-

diated n times by a pulse laser light with the duration time t_p, the luminescence intensity $I_{cw}(t_p)$ recorded with the multichannel detector during nt_p is expressed in terms of the emission intensity $I(t)$ in Eq. (1) as

$$I_{cw}(t_p) = \sum_{k=1}^{n} \left[\int_0^{t_p} I(t)dt \right] + \sum_{k=2}^{n} \left[(k-1) \int_{t_p}^{\infty} I(t)dt \right] \tag{A1}$$

$$= I_{cw,f}(t_p) + I_{cw,s}(t_p) \tag{A2}$$

$$\approx I_{cw,s}(t_p), \tag{A3}$$

where

$$I_{cw,f}(t_p) = nA_f\tau_f \left[1 + \frac{1}{2}(n-3)\exp\left(-\frac{t_p}{\tau_f} \right) \right] \tag{A4}$$

and

$$I_{cw,s}(t_p) = nA_s\tau_s \left[1 + \frac{1}{2}(n-3)\exp\left(-\frac{t_p}{\tau_s} \right) \right]. \tag{A5}$$

The first term in Eq. (A1) represents the decay intensity of emission during the time t_p and the second term represents the remaining emission due to the preceding decay.

In cw measurement, one cannot neglect the second term in Eq. (A1) that is accumulated to the net intensity of the emission, and the contribution of the fast component, $I_{cw,f}(t_p)$, to $I_{cw}(t_p)$ is negligibly small compared to that of the slow one, $I_{cw,s}(t_p)$, since τ_f is smaller than τ_s by two orders of the magnitude as seen from Fig. 7(a). Namely, Eq. (A3) holds practically, so one obtains only the information from the isolated F center in the cw measurement. We have confirmed experimentally that $I_e(E_{ph})$ is proportional to the $I_{cw}(t_p)$ in Eq. (A3) in the energy range from 1.9 to 2.2 eV, where the energy dependence of τ_s is available.

[1] See, e.g., B. Henderson and R. H. Bartram, *Crystal-Field Engineering of Solid-State Laser Materials* (Cambridge University Press, Cambridge, U.K., 2000); *Advances in Nonradiative Processes in Solids*, NATO Advanced Studies Institute, Series B: Physics, edited by B. Di Bartolo (Plenum, New York, 1991), Vol. 249.

[2] D. L. Dexter, C. C. Klick, and G. A. Russell, Phys. Rev. **100**, 603 (1955).

[3] H. Fedders, M. Hunger, and F. Lüty, J. Phys. Chem. Solids **22**, 299 (1961).

[4] A. Miehlich, Z. Phys. **176**, 168 (1963).

[5] F. Porret and F. Lüty, Phys. Rev. Lett. **26**, 843 (1971).

[6] S. Honda and M. Tomura, J. Phys. Soc. Jpn. **33**, 1003 (1972).

[7] G. Baldacchini, D. S. Pan, and F. Lüty, Phys. Rev. B **24**, 2174 (1981).

[8] S. Wakita, Y. Suzuki, and M. Hirai, J. Phys. Soc. Jpn. **50**, 2781 (1981).

[9] M. Hirai and S. Wakita, Semicond. Insul. **5**, 231 (1983).

[10] K. Asami, T. Naka, and M. Ishiguro, Phys. Rev. B **34**, 5658 (1986).

[11] G. Baldacchini, in *Advances in Nonradiative Processes in Solids*, edited by B. Di Bartolo (Plenum, New York, 1989), pp. 219–259.

[12] F. DeMatteis, M. Leblans, and D. Schoemaker, Phys. Rev. B **49**, 9357 (1994).

[13] F. DeMatteis, M. Leblans, W. Slootmans, and D. Schoemaker, Phys. Rev. B **50**, 13186 (1994).

[14] G. Baldacchini, Proc. SPIE **3176**, 142 (1997).

[15] U. M. Grassano, in *Advances in Nonradiative Processes in Solids*, edited by B. Di Bartolo (Plenum, New York, 1989), pp. 331–351.

[16] J. DeKinder, W. Joosen, and D. Schoemaker, Phys. Rev. B **42**, 9674 (1990).

[17] M. Nisoli, S. DeSilvestri, O. Svelto, R. Scholz, R. Fanciulli, V. Pellegrini, F. Beltram, and F. Bassani, Phys. Rev. Lett. **77**, 3463 (1996).

[18] R. Scholz, M. Schreiber, F. Bassani, M. Nisoli, S. De Silvestri, and O. Svelto, Phys. Rev. B **56**, 1179 (1997).

[19] N. Akiyama and S. Muramatsu, Phys. Rev. B **67**, 125115 (2003).

[20] T. Koyama, Y. Takahashi, M. Nakajima, and T. Suemoto, Phys. Rev. B **76**, 115122 (2007).

[21] T. Koyama, M. Nakajima, and T. Suemoto, Phys. Rev. B **78**, 155126 (2008).

[22] R. H. Bartram and A. M. Stoneham, Solid State Commun. **17**, 1593 (1975).

[23] C. H. Leung and K. S. Song, Solid State Commun. **33**, 907 (1980).

[24] H. Sumi, Solid State Commun. **43**, 73 (1982).

[25] R. H. Bartram and A. M. Stoneham, Semicond. Insul. **5**, 297 (1983).

[26] R. H. Bartram, J. Phys. Chem. Solids **51**, 641 (1990).

[27] Y. Kayanuma, J. Phys. Soc. Jpn. **57**, 292 (1988).

[28] M. Hama and M. Aihara, Phys. Rev. B **38**, 1221 (1988).

[29] Y. Farge and M. P. Fontana, *Ionic Crystals* (North-Holland, Amsterdam, 1979).

[30] W. B. Fowler, in *Physics of Color Centers*, edited by W. B. Fowler (Academic, New York, 1968), Chap. 2.

[31] N. Akiyama and H. Ohkura, Phys. Rev. B **53**, 10632 (1996).

[32] F. Lüty, in *Physics of Color Centers*, edited by W. B. Fowler (Academic, New York, 1968), Chap. 3.

[33] N. Akiyama, S. Muramatsu, M. Arai, K. Nakamura, and G. Baldacchini, J. Lumin. **109**, 155 (2004).

[34] N. Akiyama, S. Muramatsu, and G. Baldacchini, J. Lumin. **128**, 504 (2008).

[35] M. Fox, *Optical Properties of Solids* (Oxford University Press, Oxford, U.K., 2001), p. 94.

[36] P. Raerinne, Meas. Sci. Technol. **3**, 75 (1992).

[37] D. Fröhlich and H. Mahr, Phys. Rev. **148**, 868 (1966).

[38] L. Bosi, C. Bussolati, and G. Spinolo, Phys. Rev. B **1**, 890 (1970).

[39] D. Fröhlich and H. Mahr, Phys. Rev. **141**, 692 (1966).

[40] R. K. Swank and F. C. Brown, Phys. Rev. **130**, 34 (1963).

[41] K. Park, Phys. Rev. **140**, A1735 (1965).
[42] G. Chiarotti and U. M. Grassano, Phys. Rev. Lett. **16**, 124 (1966).
[43] S. Benci and M. Manfredi, Phys. Rev. B **7**, 1549 (1973).
[44] L. Bosi, A. Longoni, and M. Nimis, Phys. Status Solidi B **89**, 221 (1978).
[45] See example in Ref. 35. At low temperatures the inverse of the lifetime τ is given by $\frac{1}{\tau}=1/\tau_R+1/\tau_{NR}$, where τ_{NR} denotes a nonradiative lifetime.
[46] K. Huang and A. Rhys, Proc. R. Soc. London, Ser. A **204**, 406 (1950).
[47] A. M. Stoneham, *Theory of Defects in Solids* (Clarendon, Oxford, 1975), p. 548.
[48] A. M. Stoneham, *Theory of Defects in Solids* (Clarendon, Oxford, 1975), Chap. 10.
[49] W. B. Fowler, in *Physics of Color Centers*, edited by W. B. Fowler (Academic, New York, 1968), p. 627.